Complex Behavior in Coupled Bromate Oscillators

Yu Chen and Jichang Wang*

Department of Chemistry and Biochemistry, The University of Windsor, Windsor, ON N9B 3P4, Canada

Received: February 11, 2005; In Final Form: March 16, 2005

In this study, coupled bromate-oscillators constructed by adding 1,4-cyclohexanedione (1,4-CHD) to the ferroin-catalyzed Belousov−Zhabotinsky reaction are investigated in a batch reactor under anaerobic conditions. Various complex behaviors such as sequential oscillations and bursting phenomena are observed. At low concentrations of ferroin or malonic acid (MA), the development of sequential oscillations is found to depend on the ratio of [1,4-CHD]/[ferroin] and [1,4-CHD]/[MA] rather than their absolute concentrations. As the concentration of MA or ferroin was increased gradually, however, the minimum 1,4-CHD concentration required to induce complex oscillations reaches a plateau. Perturbations by light illustrate that the first oscillatory window is governed by the ferroin−MA−BZ mechanism, whereas the 1,4-CHD−bromate oscillator plays a prominent role during the non-oscillatory evolution and the second oscillatory window. Our conclusion is further supported by numerical simulations in which sequential oscillations observed in experiments are qualitatively reproduced by a modified FKN mechanism.

1. Introduction

As one of the best understood chemical oscillators,[1−13] the Belousov−Zhabotinsky (BZ) reaction has been frequently employed as a model system to gain insight into various nonlinear spatiotemporal behaviors.[14−26] For example, spatially extended BZ reactions catalyzed by ferroin or ruthenium have been investigated extensively in the past two decades, which led to observations of various types of pattern formation.[27−31] The classic BZ reaction is the oxidation and bromination of organic substrates, malonic acid (MA), by acidic bromate in the presence of metal ion catalyst.[1] When MA was replaced by a different organic substrate or when two or more substrates are present simultaneously, the BZ reaction is found to exhibit quite different nonlinear behavior, including the occurrence of complex oscillations and/or dramatic changes in the frequency and amplitude of oscillation.[32−37]

In this study, we investigated the oscillatory behavior of the ferroin-catalyzed BZ reaction in the presence of a second substrate, 1,4-cyclohexanedione (1,4-CHD). As reported in the literature,[5] 1,4-CHD alone is capable of forming a chemical oscillator with bromate in an acidic environment. Therefore, in addition to a new route of regenerating reduced metal catalysts (i.e. ferroin), the presence of 1,4-CHD in the ferroin−MA−bromate reaction also implements new autocatalytic feedbacks, such as reactions of hydroquinone and bromine dioxide radicals.[38,39] As a result, the mixed BZ system studied here consists of two bromate oscillators that are coupled together through such reagents as bromine dioxide, ferroin/ferriin, bromine, etc. Forming a coupled oscillatory system is an essential difference between this study and earlier investigations of BZ reactions using two or more organic substrates,[32−37] in which kinetic effects are mainly caused by competitions on the regeneration of ferroin. As shown in the following, the presence of coupled nonlinear feedbacks leads to the occurrence of non-oscillatory evolution and bursting phenomena. Interestingly, the critical coupling strength (i.e., the ratio of [1,4-CHD]/[MA] and [1,4-CHD]/[ferroin]) reaches a plateau as the initial concentration of MA or ferroin is increased continuously.

2. Experimental Procedures

All reactions were carried out in a thermostated cylindrical glass vessel, where temperature was controlled at (25.0 ± 0.1) °C by a circulating water bath (Fisher Scientific). The volume of the reaction mixture was kept constant at 30.0 mL throughout this study. There was about a 1-cm gap between the solution and the bottom of a Teflon lid. To avoid the influence of oxygen, nitrogen gas was continuously flowed into the gap at a speed of about 0.05 L/min. To examine whether flowing inert gases above the solution surface affects the reaction kinetics, for example, via inducing the loss of volatile species such as bromine, etc., argon was supplied at a much lower flow rate and no difference in the behavior was recorded. Reactions were followed by a platinum electrode coupled with a $Hg|Hg_2SO_4|K_2SO_4$ reference electrode. A personnel computer, interfaced through a PowerLab/4SP instrument (ADInstruments), was used to collect Pt potentials.

For experiments illuminated by light, a fiber-optic halogen lamp (Fisher Scientific, Model DLS-100HD, 150W) with dual bifurcated fibers and continuously variable light levels was used as the light source. The two optical fibers were positioned at the opposite sides of the cylindrical glass reactor and about 1 cm away from the external wall of the reactor. The light intensity was measured with an optical photometer from Newport. No temperature change was observed when the reaction mixture was illuminated by light, indicating that observed effects were caused by photochemical reactions.

Stock solutions of $NaBrO_3$ (Aldrich, 99%; 1.0 M), malonic acid (Aldrich, 98%; 0.8 M), and H_2SO_4 (Aldrich, 98%; 3 M) were prepared in double-distilled water. Ferroin ($Fe(phen)_3^{2+}$), 0.025 M, was prepared with $FeSO_4 \cdot 7H_2O$ (Aldrich) and 1,10-phenanthroline (Aldrich) according to a 1:3 stoichiometric relationship. 1,4-CHD (Aldrich, 98%) was directly dissolved in the reaction mixture. Bromate solution was added to the

* Address correspondence to this author. E-mail: jwang@uwindsor.ca. Fax: 1-519-973-7098.

10.1021/jp050756q CCC: $30.25
Published on Web 04/12/2005

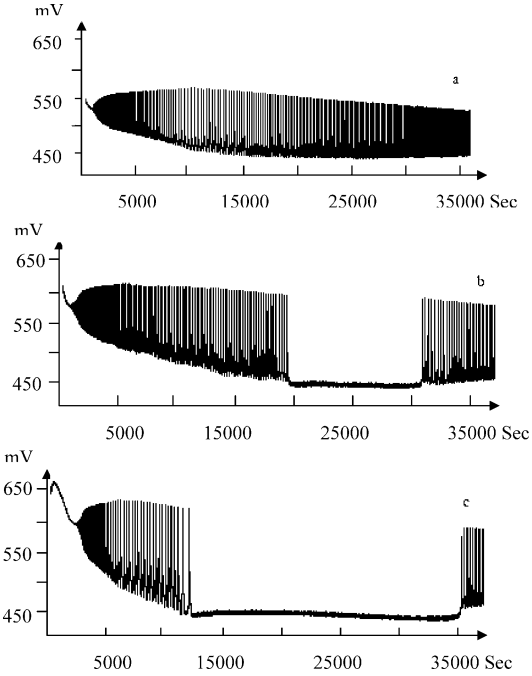

Figure 1. Time series showing the evolution of the mixed BZ reaction under different initial concentrations of 1,4-CHD: (a) 0.008, (b) 0.010, and (c) 0.015 M. Initial values of other reactants are $[H_2SO_4] = 0.4$ M, [MA] = 0.085 M, [ferroin] = 4.0×10^{-4} M, and $[BrO_3^-] = 0.08$ M.

reaction solution after 1,4-CHD had dissolved completely. All chemicals used here were commercial grade and were used without further purification. Influences of initial concentrations of 1,4-CHD, MA, BrO_3^-, and ferroin on the reaction dynamics have been studied here, in which their concentrations were adjusted respectively within the following ranges: 0.015−0.08 M (1,4-CHD), 0.075−0.25 M (MA), 0.07−0.09 M (BrO_3^-), and 3.0×10^{-4}−8.0×10^{-4} M (ferroin).

3. Experimental Results

Figure 1 presents three time series of the mixed BZ reaction conducted at different initial concentrations of 1,4-CHD: (a) 0.008, (b) 0.010, and (c) 0.015 M. Other reaction conditions are $[H_2SO_4] = 0.4$ M, [MA] = 0.085 M, $[Fe(phen)_3^{2+}] = 4.0 \times 10^{-4}$ M, and $[BrO_3^-] = 0.08$ M. As is shown in the figure, there was a long induction time (>700 s), which grows as 1,4-CHD concentration is increased. In the absence of 1,4-CHD, the induction time is shorter than 80 s. During the induction period, the color of the reaction solution is blue, indicating that the system is in an oxidized state (i.e., high $Fe(phen)_3^{3+}$ concentration). The smooth growth in the amplitude of these oscillations suggests that the system undergoes a supercritical Hopf-bifurcation. In Figure 1a, only a small amount of 1,4-CHD is added, and modulations in the frequency of oscillation can be seen at around 10 000 s after mixing all reactants together. As 1,4-CHD concentration is increased, more dramatic changes in the reaction behavior appear in Figure 1b, in which a long quiescent period develops in the middle of the oscillatory window. Such a behavior resembles sequential oscillations reported in earlier investigations. The non-oscillatory evolution commenced earlier and lasted longer if 1,4-CHD concentration was increased still (see Figure 1c), suggesting that 1,4-CHD plays an important role in the development of the sequential oscillations. In Figure 2, the length of the non-oscillatory period is plotted as a function of the initial concentration of 1,4-CHD, in which the period of the non-oscillatory window increases

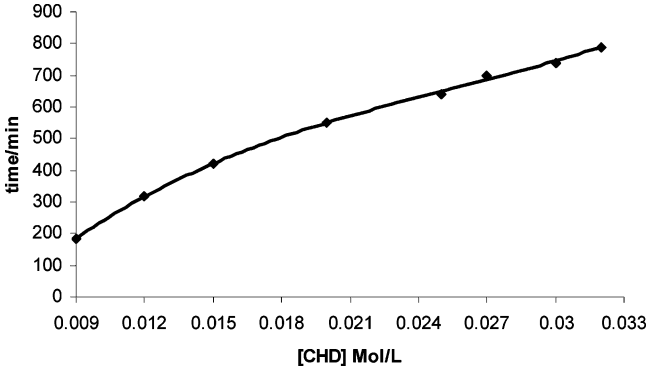

Figure 2. Dependence of the non-oscillatory evolution on the initial concentration of 1,4-CHD. Other reaction conditions are $[H_2SO_4] = 0.4$ M, [MA] = 0.085 M, [ferroin] = 4.0×10^{-4} M, and $[BrO_3^-] = 0.08$ M. The *y*-axis indicates how long the non-oscillatory evolution lasts. A linear relationship can be seen here.

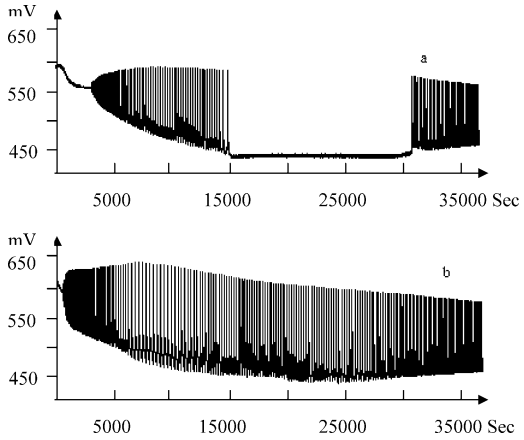

Figure 3. Time series of the mixed BZ reaction under different initial concentrations of ferroin: (a) 3.0×10^{-4} and (b) 8.0×10^{-4} M. Initial compositions of other reactants are $[H_2SO_4] = 0.4$ M, [MA] = 0.085 M, [1,4-CHD] = 0.01 M, and $[BrO_3^-] = 0.08$ M. Transitions between simple and complex oscillations appear under this set of reaction conditions.

nearly linearly with the 1,4-CHD concentration. It is important to point out that as 1,4-CHD concentration is increased, both the first and the second group of oscillations last for a shorter period of time and their amplitudes also become smaller. When 1,4-CHD concentration is increased to 0.032 M, only two peaks with an extremely slow oscillation frequency are obtained in the second oscillatory window.

The above influences of 1,4-CHD on reaction behavior could arise from two sources: (1) 1,4-CHD competes with MA to react with ferriin, bromine, etc., and (2) the 1,4-CHD oscillator competes with the classic BZ oscillator for the autocatalyst, bromine dioxide radicals. If competitions for bromine dioxide radicals played an important role in inducing the non-oscillatory evolution, similar effects of increasing 1,4-CHD concentration should be achieved by decreasing the concentration of ferroin. In Figure 3, two time series of the mixed BZ reaction are shown at (a) $[Fe(phen)_3^{2+}] = 3.0 \times 10^{-4}$ M and (b) $[Fe(phen)_3^{2+}] = 8.0 \times 10^{-4}$M. Other reaction conditions were $[H_2SO_4] = 0.4$ M, [MA] = 0.085 M, [1,4-CHD] = 0.01 M, and $[BrO_3^-] = 0.08$ M. This figure shows that increasing ferroin concentration does exhibit opposite effects as increasing 1,4-CHD concentration on the development of sequential oscillations. Therefore, as suggested earlier, competitions of the two bromate-based oscillators through the autocatalytic processes appear to play an essential role in the occurrence of sequential oscillations.

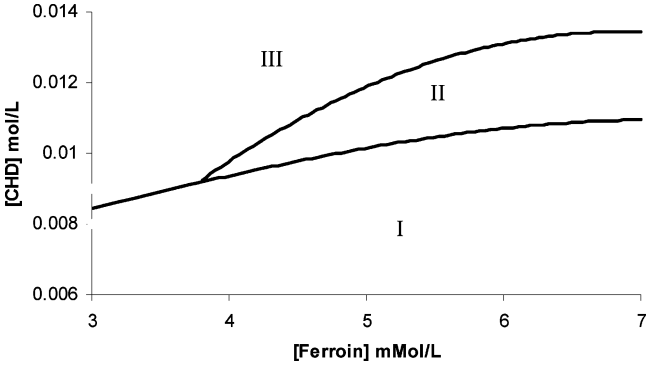

Figure 4. Phase diagram showing complex reaction dynamics in the 1,4-CHD−ferroin concentration phase plane. Other reaction conditions are $[H_2SO_4] = 0.4$ M, [MA] = 0.085 M, and $[BrO_3^-] = 0.08$ M.

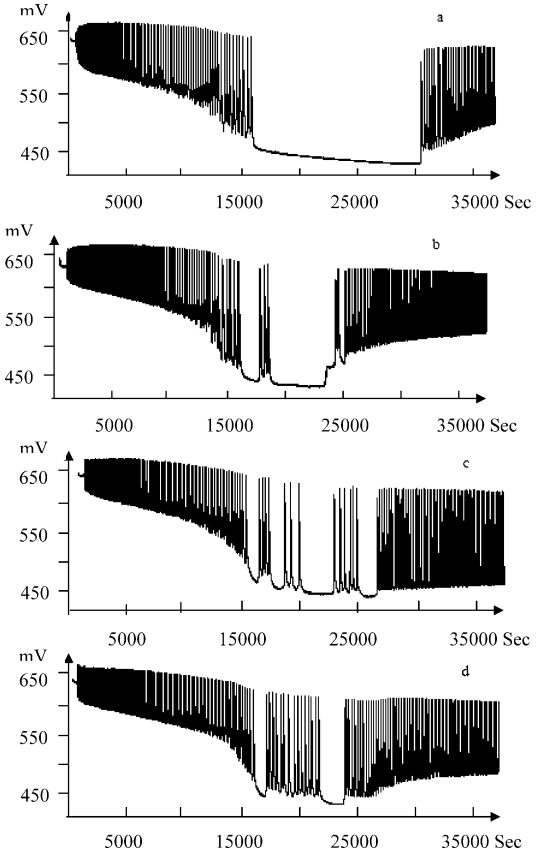

Figure 5. Time series of the coupled BZ reaction under different initial concentrations of malonic acid: (a) 0.1, (b) 0.2, (c) 0.25, and (d) 0.3 M. Other reaction conditions are $[H_2SO_4] = 0.4$ M, [1,4-CHD] = 0.012 M, [ferroin] = 4.0×10^{-4} M, and $[BrO_3^-] = 0.08$ M.

Figure 4 presents a phase diagram of the reaction dynamics in the ferroin−1,4-CHD concentration plane, in which three dynamic areas are observed: (I) simple oscillations, (II) bursting phenomena (such as shown in Figure 5c), and (III) sequential oscillations. When the ratio of [1,4-CHD]/[ferroin] is low (i.e., in region I), only one oscillatory window similar to those shown in Figures 1a and 2b is observed. The threshold ratio of [1,4-CHD]/[ferroin] for transition from simple to complex oscillations is nearly constant over a broad range, indicating that the ratio of [1,4-CHD]/[ferroin] is more important than their absolute concentrations. However, as the concentration of ferroin moves to a higher region, the threshold concentration of 1,4-CHD appears to reach a plateau. In addition, at high ferroin concentration, increasing the concentration of 1,4-CHD will cause the system to exhibit bursting phenomena first, and then the system moves to the parameter region where only sequential oscillations can be seen.

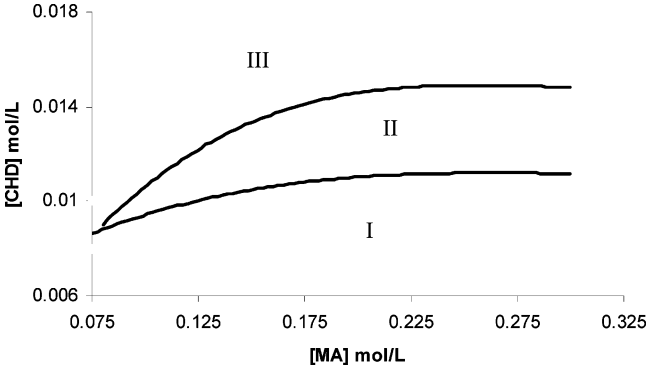

Figure 6. Phase diagram showing the reaction dynamics in the 1,4-CHD−MA concentration phase plane. Other reaction conditions are $[H_2SO_4] = 0.4$ M, [ferroin] = 4.0×10^{-4} M, and $[BrO_3^-] = 0.08$ M.

Figure 5 shows four time series achieved under different initial concentrations of MA: (a) 0.10, (b) 0.20, (c) 0.25, and (d) 0.30 M. Other reaction conditions are $[H_2SO_4] = 0.4$ M, $[Fe(phen)_3^{2+}] = 4.0 \times 10^{-4}$ M, [1,4-CHD] = 0.012 M, and $[BrO_3^-] = 0.08$ M. Notably, complex oscillatory behavior is observed for all four experiments in which MA concentration triples. This result illustrates that the effect of MA on the dynamics of the mixed BZ system is not as dramatic as that of 1,4-CHD. In other words, competitions between 1,4-CHD and MA for reagents such as bromine, ferriin, etc. are not critical in the development of the non-oscillatory window. However, as the concentration of MA is doubled to 0.2 M, a new complex phenomenon resembling bursting oscillations occurs within the non-oscillatory window (e.g., between 15 000 and 30 000 s). Bursting oscillations appear to occur more frequently as the concentration of MA acid is increased further (see Figure 5c). Eventually, the bursting oscillations combine to form one large group of oscillations (Figure 5d), which leads to three isolated oscillatory windows.

In Figure 6, complex oscillations are characterized in the 1,4-CHD−MA concentration phase plane. Other reaction conditions are $[H_2SO_4] = 0.4$ M, $[Fe(phen)_3^{2+}] = 4.0 \times 10^{-4}$ M, and $[BrO_3^-] = 0.08$ M. Three dynamic regions are observed. Only simple oscillations with one oscillatory window are observed in region I, whereas complex reaction behavior is seen in both region II (sequential oscillations) and region III (burst phenomena). It is interesting to note that at low MA concentration, the threshold 1,4-CHD concentration required to induce complex oscillations also appears to increase proportionally with respect to an increase in the initial concentration of MA. Whether such a relationship between [1,4-CHD] and [MA] arises from their competitions for ferroin or reactions with bromine remains to be understood. Nevertheless, the above phase diagram illustrates that interactions of 1,4-CHD and MA play an important role in the development of bursting phenomena, especially under low MA concentrations.

In addition to those reactants which are known to be involved in reactions competing with 1,4-CHD and/or products of 1,4-CHD, bromate and sulfuric acid are also investigated in this study. Figure 7 presents two time series obtained under different initial concentrations of bromate: (a) 0.07 and (b) 0.09 M. All other reaction conditions are the same as those in Figure 1b. Compared with the result shown in Figure 1b, the non-oscillatory window appeared earlier and lasted for a much longer time in Figure 7a as a result of the decreased bromate concentration. On the other hand, when the concentration of bromate is

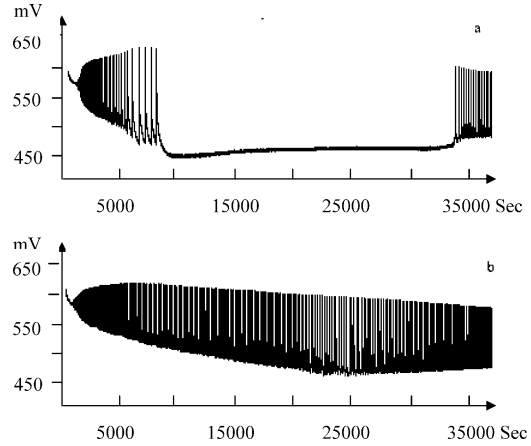

Figure 7. Time series of the coupled BZ reaction under different initial concentrations of bromate: (a) 0.07 and (b) 0.09 M. Other reaction conditions are $[H_2SO_4] = 0.4$ M, [1,4-CHD] = 0.01 M, [ferroin] = 4.0×10^{-4} M, and [MA] = 0.085 M.

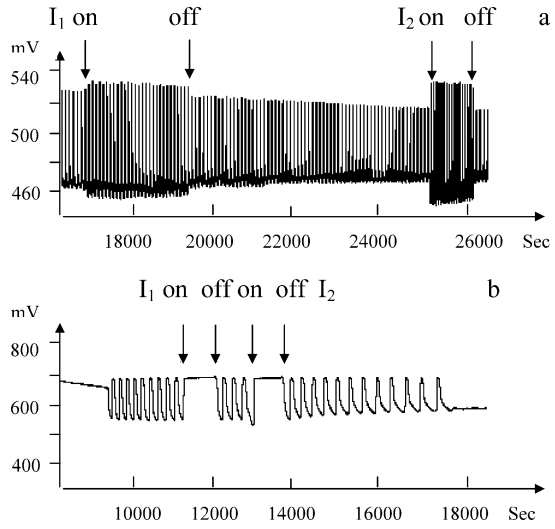

Figure 8. (a) Photoresponses of the ferroin−MA−bromate oscillations, in which initial compositions of the reaction solutions are $[H_2SO_4] = 0.4$ M, [MA] = 0.085 M, [ferroin] = 4.0×10^{-4} M, and $[BrO_3^-] = 0.08$ M; (b) photoresponses of the 1,4-CHD−bromate oscillations, where initial compositions of the reaction mixture are $[H_2SO_4] = 0.4$ M, [1,4-CHD] = 0.01 M, and $[BrO_3^-] = 0.08$ M. $I_1 = 50$ mW/cm^2, and $I_2 = 100$ mW/cm^2.

increased, only modulations in the frequency of oscillation are seen in Figure 7b. If the initial concentration of sulfuric acid is increased to 0.5 M with all other conditions the same as in Figure 1b, complex oscillations disappeared; on the other hand, if the sulfuric acid concentration is decreased to 0.3 M, the non-oscillatory window appears earlier and lasts for a longer period of time, similar to the effect of decreasing bromate concentration.

Earlier studies have demonstrated that the 1,4-CHD−bromate oscillator generally has a long induction time (>30 min).[5,38] Therefore, oscillations of the first oscillatory window are presumably governed by the classic BZ reaction mechanism. To shed light on properties of the nonoscillatory evolution and the second oscillatory window, illumination was employed as a means to perturb the mixed BZ reaction. According to existing literature,[40−43] the ferroin-catalyzed BZ reaction and the 1,4-CHD−bromate oscillator respond differently to light perturbation. Figure 8 presents the photoresponses of the ferroin−BZ oscillator (time series a) and the 1,4-CHD−ferroin−bromate oscillator (time series b). As shown in Figure 8a, under the

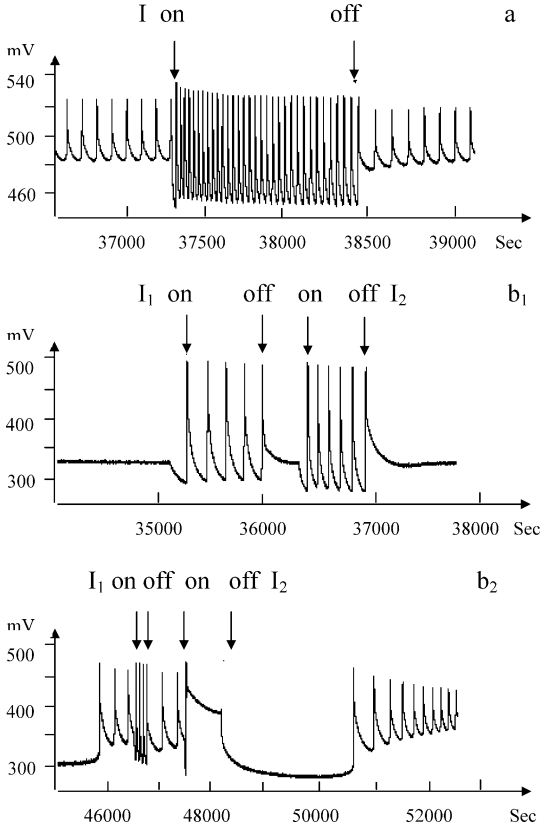

Figure 9. Photoresponses of the mixed BZ reaction at different initial concentrations of 1,4-CHD: (a) 0.01 and (b) 0.02 M. Other reaction conditions are $[H_2SO_4] = 0.4$ M, [MA] = 0.085 M, [ferroin] = 4.0×10^{-4} M, and $[BrO_3^-] = 0.08$ M. $I_1 = 50$mW/cm^2, and $I_2 = 100$ mW/cm^2.

conditions studied here, the ferroin-catalyzed BZ reaction responds to illumination with significant increases in both the amplitude and frequency of oscillation. Furthermore, quenching is not achieved even when the intensity of the applied light is increased to 100 mW/cm^2. The above constructive impacts of light could result from light-induced production of bromous acid and/or photoreduction of $Fe(phen)_3^{2+}$.[31,40] On the other hand, quenching behavior is observed in the 1,4-CHD−bromate−ferroin system when the applied light intensity exceeds 50 mW/cm^2. The two bromate-driven oscillators studied here have opposite responses to illumination.

Responses of the mixed BZ system to light perturbation are shown in Figure 9, in which the concentration of 1,4-CHD is varied: (a) 0.01 and (b) 0.02 M. Figure 9a shows that when light was used to perturb the second oscillatory window, significant amplifications in the amplitude and frequency of oscillation took place. Those variations are similar to what occurred in Figure 8a. Notably, no quenching behavior was observed even after the light intensity was increased to 100 mW/cm^2. This result suggests that oscillations within the second oscillatory window are still dominated by the classic BZ reaction mechanism. Perturbations on the non-oscillatory window did not produce any interesting behavior, where no light-induced oscillations were observed. As the initial concentration of 1,4-CHD was increased to 0.02 M, significant changes in photosensitivity took place at the latter stage of the non-oscillatory window, where light-induced oscillations were observed (see Figure 9b1). Frequencies of those light-induced oscillations increase with respect to the intensity of the applied light. Such a scenario is qualitatively the same as what was reported in the 1,4-CHD−bromate−ferroin reaction system.[41]

As shown in Figure 9b2, within the second oscillatory window illumination with 50 mW/cm^2 light was able to amplify both the amplitude and frequency of oscillation. Such a behavior is the same as what appeared in the classic BZ oscillator (see Figure 8a). However, as the light intensity is increased to 100 mW/cm^2 quenching phenomena are observed. Such qualitative changes in responses to light have been reported in the 1,4-CHD−bromate and the 1,4-CHD−bromate−ferroin systems,[41,42] but not in the classic ferroin−BZ reaction. The above experiments thus suggest that, as the initial concentration of 1,4-CHD is increased, the 1,4-CHD−bromate oscillator plays an increasingly important role in the non-oscillatory evolution and in the second oscillatory window.

4. Computational Results

Our model is constructed by combining a mechanism proposed by Strizhak and co-workers[44] for the ferroin-catalyzed BZ reaction and a model developed by Körös and co-workers[38] for the 1,4-CHD-bromate system. The complete model (Table 1) consists of 43 reaction steps and 17 variables. Most of the rate constants are taken from the literature without modification.[38,39,44]

Figure 10 presents three time series calculated from the model listed in Table 1, in which the initial concentration of 1,4-CHD is adjusted as the only variable: (a) 0.004, (b) 0.010, and (c) 0.015 M. Similar to experimental observation, there is only one oscillatory window when the concentration of 1,4-CHD is low. When [1,4-CHD] is increased to 0.010 M, a long period of non-oscillatory evolution occurs, separating the oscillations into two parts. This result supports that the complex oscillations seen in experiments arise from intrinsic reaction dynamics. Consistent with experimental observation, in the simulation the induction time of these spontaneous oscillations also increases with respect to 1,4-CHD concentration. While the model was able to qualitatively reproduce sequential oscillations induced by the presence of 1,4-CHD, influences of 1,4-CHD on the duration of the non-oscillatory evolution could not be reproduced. Specifically, further increasing 1,4-CHD concentration in the modeling (see Figure 10, parts b and c) does not prolong the non-oscillatory period as seen in experiments (see Figure 2). Further improvement of the model will be pursued in our future work.

To decipher the governing mechanisms in each reaction stage, during the simulation process we temporarily eliminated one of the two suboscillators. These calculations show that, within the first oscillatory window, if concentrations of MA and BrMA are set to zero (i.e., to remove the ferroin−BZ oscillator), spontaneous oscillations stop immediately; however, temporarily setting concentrations of 1,4-CHD and BrCHD to zero does not affect those spontaneous oscillations. This illustrates that the first oscillatory window is indeed governed by the classic BZ oscillator. During the non-oscillatory period, if concentrations of 1,4-CHD and BrCHD are set to zero, spontaneous oscillations reappear immediately, illustrating that the 1,4-CHD−bromate reactions play an essential role in the occurrence of the non-oscillatory window. If concentrations of MA and BrMA are temporarily set to zero within the non-oscillatory window, no spontaneous oscillations could appear unless the concentration of 1,4-CHD is increased slightly. Close examination reveals that this is because most of the 1,4-CHD is converted to BrCHD during the first oscillatory window. Indeed, during the non-oscillatory window, temporarily setting BrCHD concentration to zero alone will be sufficient to revive oscillatory behavior. This suggests that BrCHD dominates the production of bromide at a rate that is sufficient to quench oscillatory behavior.

TABLE 1

no.	reaction	rate constant
	A. reactions between bromine-containing compounds	
1	$Br^- + BrO_3^- + 2H^+ \rightarrow HOBr + HBrO_2$	0.1[a]
2	$HOBr + HBrO_2 \rightarrow Br^- + BrO_3^- + 2H^+$	3.3
3	$HBrO_2 + Br^- + H^+ \rightarrow 2HOBr$	1.6×10^6
4	$2HOBr \rightarrow HBrO_2 + Br^- + H^+$	2×10^{-5}
5	$HOBr + Br^- + H^+ \rightarrow Br_2 + H_2O$	1.84×10^9
6	$Br_2 + H_2O \rightarrow HOBr + Br\text{-} + H^+$	*b*
7	$2HBrO_2 \rightarrow BrO_3^- + HOBr + H^+$	3000
8	$BrO_3^- + HOBr + H^+ \rightarrow 2HBrO_2$	6.0×10^{-9}
9	$BrO_3^- + HBrO2 + H^+ \rightarrow 2BrO_2^\bullet + H_2O$	40
10	$2BrO_2^\bullet + H_2O \rightarrow BrO_3^- + HBrO_2 + H^+$	4.2×10^7
	B. reactions with the participation of bromine-containing compounds and malonic acid derivatives	
11	$MA + Br_2 \rightarrow BrMA + Br^- + H^+$	28.65
12	$MA + HOBr \rightarrow BrMA + H_2O$	8.2
13	$BrMA + HOBr \rightarrow$ product	0.1
14	$2BrMA^\bullet + H_2O \rightarrow BrMA + BrTTA$	1×10^8
15	$BrMA^\bullet + BrO_2^\bullet + H_2O \rightarrow HBrO_2 + BrTTA$	5×10^9
16	$BrMA^\bullet + MA^\bullet + H_2O \rightarrow MA + BrTTA$	1×10^9
17	$MA^\bullet + BrO_2^\bullet \rightarrow$ product	5×10^9
18	$MA^\bullet + BrO_3^- + H^+ \rightarrow BrO_2^\bullet +$ product	32
19	$BrTTA \rightarrow Br^-$ + product	*c*
20	$BrMA^\bullet + BrO_3^- + H^+ \rightarrow BrO_2^\bullet + BrTTA$	32
	C. reactions with the participation of the catalyst	
21	$Fe^{2+} + BrO_2^\bullet + H^+ \rightarrow Fe^{3+} + HBrO_2$	10×10^8
22	$2Fe^{2+} + BrO_3^- + 3H^+ \rightarrow 2Fe^{3+} + HBrO_2 + H_2O$	0.256
23	$2Fe^{2+} + HBrO_2 + 2H^+ \rightarrow 2Fe^{3+} + HOBr + H_2O$	1.6
24	$2Fe^{2+} + HOBr + H^+ \rightarrow 2Fe^{3+} + Br^- + H_2O$	5×10^{-3}
25	$2Fe^{2+} + Br_2 + H^+ \rightarrow 2Fe^{3+} + 2Br^-$	100
26	$2Fe^{3+} + 2Br^- \rightarrow 2Fe^{2+} + Br_2 + H^+$	see ref 26
27	$Fe^{3+} + MA \rightarrow Fe^{2+} + MA^\bullet + H^+$	1×10^{-2}
28	$Fe^{3+} + BrMA \rightarrow Fe^{2+} + BrMA^\bullet + H^+$	20
29	$Fe^{2+} + BrMA^\bullet + H^+ \rightarrow Fe^{3+} + BrMA$	3.2×10^9
	D. reactions with 1,4-CHD	
30	$H_2Q + 2BrO_2^\bullet \rightarrow 2HBrO_2 + Q$	2×10^6
31	$H_2Q + Br_2 \rightarrow Q + 2Br^-$	1×10^4
32	$H_2Q + H^+ + BrO_3^- \rightarrow Q + HBrO_2 + H_2O$	1.6×10^{-2}
33	$H_2Q + HOBr \rightarrow Q + Br^- + H^+ + H_2O$	6×10^5
34	$H_2Q + 2Fe^{3+} \rightarrow 2Fe^{2+} + Q + 2H^+$	6×10^3
35	$CHD + H^+ \rightarrow CHDE + H^+$	2.1×10^{-4}
36	$CHDE + H^+ \rightarrow CHD + H^+$	5.2×10^2
37	$CHDE + Br_2 \rightarrow BrCHD + H^+ + Br^-$	2.8×10^9
38	$CHD + HBrO_2 \rightarrow H_2Q + HOBr + H_2O$	5
39	$BrCHD + H^+ \rightarrow CHED + Br^- + 2H^+$	5×10^{-5}
40	$CHED + H^+ \rightarrow H_2Q + H^+$	8×10^{-5} [a]
41	$CHD + BrO_3^- + H^+ \rightarrow H_2Q + HBrO_2 + H_2O$	1.6×10^{-5}
42	$2Fe^{3+} + CHD \rightarrow 2Fe^{2+} + H_2Q + 2H^+$	0.03[a]
43	$2Fe^{3+} + BrCHD \rightarrow Q + Br^- + 3H^+ + 2Fe^{2+}$	0.051

[a] Indicates that the value used here is different from what was used in ref 38. [b] Discussion regarding the election of these rate constants can be found in ref 38. [c] The concentrations of $[H^+] = 0.8$ M and $[H_2O] = 55.56$ M are included in the rate constants.

Within the second oscillatory window, spontaneous oscillations stop when concentrations of MA and BrMA are set to zero (i.e. eliminating the classic BZ reaction); on the other hand, when concentrations of 1,4-CHD and BrCHD are set to zero, oscillatory behavior lasts for a little longer time. This indicates that the classic BZ reaction still plays an essential role in the second oscillatory window, but the presence of BrCHD exerts important influences on the oscillatory behavior. This conclusion is consistent with the experimental observation that the second oscillatory window exhibits subtle responses to light perturbation, in which BrCHD may lead to additional production of Br^- and consequently result in light-induced quenching phenomena.

5. Conclusions

This study investigates the nonlinear dynamics of a mixed BZ reaction system, in which there are two organic substrates,

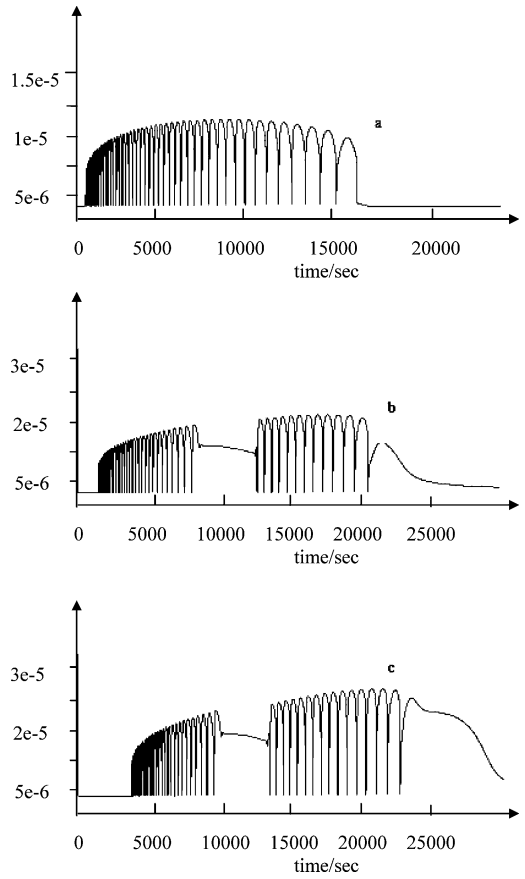

Figure 10. Time series calculated from the model under different initial concentrations of 1,4-CHD: (a) 0.004, (b) 0.01, and (c) 0.015 M. Other initial conditions are $[H_2SO_4] = 0.4$ M, $[MA] = 0.085$ M, $[Fe(phen)_3^{2+}] = 4.0 \times 10^{-4}$ M, $[BrO_3^-] = 0.08$ M, and $[Br^-] = 1 \times 10^{-8}$ M. Initial concentrations of other intermediate species are set to zero. Rate constants used in these calculations are provided in Table 1.

namely, 1,4-CHD and MA. As opposed to the vast majority of previous studies with mixed substrates,[32−37] in this study the second organic substrate, 1,4-CHD, not only participates in reactions which compete with the first substrate, but also introduces an additional nonlinear feedback. As is shown in Figures 1−6, complex behavior such as sequential oscillations and bursting phenomena is induced by the presence of the second substrate. The fact that concentrations of 1,4-CHD and ferroin exhibit opposite effects on the occurrence of a non-oscillatory window suggests that coupling of reactions R1−R3 may play an essential role in the development of complex reaction dynamics in the mixed system:

$$Fe(phen)_3^{2+} + BrO_2^{\bullet} + H^+ \rightarrow Fe(phen)_3^{3+} + HBrO_2 \quad (R1)$$

$$H_2Q + BrO_2^{\bullet} + H^+ \rightarrow H_2Q^{\bullet} + HBrO_2 \quad (R2)$$

$$H_2Q^{\bullet} + BrO_2^{\bullet} + H^+ \rightarrow Q + HBrO_2 \quad (R3)$$

where hydroquinone (H_2Q) is a product of 1,4-CHD. Together with reaction 9 in Table 1, reactions R1, R2, and R3 form three coupled autocatalytic feedbacks. Dolnik and co-workers have demonstrated in the ferrocyanide−iodate−sulfite reaction that coupling the nonlinear feedback step could lead to the control of the frequency, amplitude, and existence of oscillations.[45] In complement to Dolnik's work, this study demonstrates that not only modulations in the frequency and amplitude of oscillation, but even complicated dynamical behavior can be achieved by coupling nonlinear feedbacks. It is interesting to note that the occurrence of complex oscillations also appears to depend on the ratio of [1,4-CHD]/[MA], especially at low concentration of [MA], implying that couplings through nonlinear feedbacks also play an important role in the mixed BZ reaction.

Both photoperturbation experiments and numerical simulations suggest that the 1,4-CHD−bromate reaction plays a critical role during the non-oscillatory evolution. At higher initial concentration of 1,4-CHD, behavior of the second oscillatory window is greatly affected by the 1,4-CHD−bromate oscillator, as evidenced by the subtle dependence of photosensitivity on light intensity. The unique photosensitivity, the presence of complex temporal dynamics, and visible periodic color changes in the mixed BZ reaction make it an attractive model system for exploring novel spatiotemporal behavior, in particular perturbed nonlinear dynamics. Among existing studies of coupled chemical oscillators, the coupled system was usually constructed via coupling two identical chemical systems operated at different reaction conditions.[46−48] In this study, the coupled system was formed via a combination of different oscillatory chemical reactions (i.e. through "internal" couplings). Results obtained here thus shall be useful for understanding the occurrence of complex dynamics in coupled nonlinear media.

Acknowledgment. This work was supported by the National Science and Engineering Research Council, Canada (NSERC), and the Canada Foundation for Innovation (CFI).

References and Notes

(1) Field, R. J.; Burger, M., Eds. *Oscillations and Traveling Waves in Chemical Systems*; Wiley-Interscience: New York, 1985.
(2) Epstein, I. R.; Pojman, J. A. *An Introduction to Nonlinear Chemical Dynamics*; Oxford University Press: Oxford, U.K., 1998.
(3) Orban, M.; Körös, E. *J. Phys. Chem.* **1978**, *82*, 1672.
(4) Herbine, P.; Field, R. J. *J. Phys. Chem.* **1980**, *84*, 1330.
(5) Farage, V. J.; Janjic, D. *Chem. Phys. Lett.* **1982**, *93*, 621.
(6) Gaspar, V.; Showalter, K. *J. Am. Chem. Soc.* **1987**, *109*, 4869.
(7) Simoyi, R. H.; Manyonda, M.; Masere, J.; Mtambo, M.; Ncube, I.; Patel, H.; Epstein, I. R.; Kustin, K. *J. Phys. Chem.* **1991**, *95*, 770.
(8) Rabai G.; Epstein, I. R. *J. Am. Chem. Soc.* **1992**, *114*, 1529−1530.
(9) Simoyi, R. H.; Epstein, I. R.; Kustin, K. *J. Phys. Chem.* **1994**, *98*, 551.
(10) Schreiber, I.; Hung, Y.-F.; Ross, J. *J. Phys. Chem.* **1996**, *100*, 8556.
(11) Hauser, M. J. B.; Olsen, L. F.; Bronnikova, T. V.; Schaffer, W. M. *J. Phys. Chem. B* **1997**, *101*, 5075.
(12) Masere, J.; Stewart, F.; Meehan, T.; Pojman, J. A. *Chaos* **1999**, *9*, 315.
(13) Horvath, A. K.; Nagypal, I.; Epstein, I. R. *J. Am. Chem. Soc.* **2002**, *124*, 10956.
(14) Hudson, J. L.; Hart, M.; Marinko, D. *J. Chem. Phys.* **1979**, *71*, 6104.
(15) Roux, J. C.; DeKepper, P.; Boissonate, J. *Phys. Lett. A* **1983**, 97, 168.
(16) Ali, F.; Menzinger, M. *J. Phys. Chem.* **1997**, *101*, 2304.
(17) Ruoff, P. *J. Phys. Chem.* **1993**, *97*, 6405.
(18) Field, R. J.; Körös, E.; Noyes, R. M. *J. Am. Chem. Soc.* **1972**, *94*, 8649.
(19) Kalishin, E. Yu.; Goncharenko, M. M.; Khavrus, V. A.; Strizhak, P. E. *Kinet. Catal.* **2002**, *43*, 256.
(20) Wang, J.; Sørensen, P. G.; Hynne, F. *J. Phys. Chem.* **1994**, *98*, 725.
(21) Wang, J.; Sørensen, P. G.; Hynne, F. *Z. Phys. Chem.* **1995**, *192*, 63.
(22) John, B. R.; Scott, S. K.; Thompson, B. W. *Chaos* **1997**, *7*, 350.
(23) Field, R. J.; Forsterling, H.-D. *J. Phys. Chem.* **1986**, *90*, 5400.
(24) Györgyi, L.; Rempe, S. L.; Field, R. J. *J. Phys. Chem.* **1991**, *95*, 3159.
(25) Keki, S.; Magyar, I.; Beck, M. T.; Gaspar, V. *J. Phys. Chem.* **1992**, *96*, 1725.
(26) Strizhak, P. E.; Kawczynski, A. Z. *J. Phys. Chem.* **1995**, *99*, 10830.
(27) Sevcikova, H.; Schreiber I.; Marek, M. *J. Phys. Chem.* **1996**, *100*, 19153.
(28) Maselko, J.; Showalter, K. *Nature* **1989**, *339*, 609.
(29) Kaern, M.; Menzinger, M. *J. Phys. Chem. A* **2002**, *106*, 4897.

(30) Bamforth, J. R.; Toth R.; Gaspar, V.; Scott, S. K. *Phys. Chem. Chem. Phys.* **2002**, *4*, 1299.
(31) Kapral, R.; Showalter, K., Eds. *Chemical Waves and Patterns*; Kluwer Academic Publishers: Dordrecht, The Netherlands, 1995).
(32) Heilweil, J.; Henchman, M. J.; Epstein, I. R. *J. Am. Chem. Soc*. **1979**, *101*, 3698.
(33) Rsatogi, R. P.; Misra, G. P.; Das, I.; Sharma, A. *J. Phys. Chem*. **1993**, *97*, 2571.
(34) Wittmann, M.; Stirling, P.; Bódiss, J. *Chem. Phys. Lett*. **1987**, *141*, 241.
(35) Srivastava, P. K.; Mori, Y.; Hanazaki, I. *J. Phys. Chem*. **1991**, *95*, 1636.
(36) Li, H.; Huang, X. *Chem. Phys. Lett*. **1996**, *255*, 137.
(37) Shin, S. B.; Choe, S. J.; Huh, D. S. *Bull. Korean Chem. Soc*. **2000**, *21*, 215.
(38) Szalai, I.; Körös, E. *J. Phys. Chem. A* **1998**, *102*, 6892.
(39) Szalai, I.; Kurin-Csorgei, K.; Epstein, I. R.; Orban, M. *J. Phys. Chem. A* **2003**, *107*, 10074.
(40) Gaspar, V.; Bazsa, G.; Beck, M. T. *Z. Phys. Chem.* (*Leipzig*) **1983**, *264*, 43.
(41) Huh, D. S.; Kim, H. S.; Kang, J. K.; Kim, Y. J.; Kim, D. H.; Park, S. H.; Yadav, K.; Wang, J. *Chem. Phys. Lett.* **2003**, *378*, 78.
(42) Wang, J.; Yadav, K.; Zhao, B.; Gao, Q.; Huh, D. S. *J. Chem. Phys*. **2004**, *121*, 10138.
(43) Kurin-Csörgei, K.; Zhabotinsky, A. M.; Orban, M.; Epstein, I. R. *J. Phys. Chem. A* **1997**, *101*, 6827.
(44) Kalishin, E. Yu.; Goncharenko, M. M.; Khavrus, V. A.; Strizhak, P. E. *Kinet. Catal*. **2002**, *43*, 256.
(45) Dolnik, M.; Gardner, T. S.; Epstein, I. R.; Collins, J. J. *Phys. Rev. Lett*. **1999**, *82*, 1582.
(46) Hohmann, W.; Schinor, N.; Kraus, M.; Schneider, F. W. *J. Phys. Chem. A* **1999**, *103*, 5742.
(47) Votrubova, V.; Hasal, P.; Schreiberova, L.; Marek, M. *J. Phys. Chem.* **1998**, *102*, 1318.
(48) Scott, S. K. *Chemical Chaos*; Clarendon Press: Oxford, U.K., 1991.